International Journal of Engineering

Journal Homepage: www.ije.ir

Coupling Nonlinear Element Free Galerkin and Linear Galerkin Finite Volume Solver for 2D Modeling of Local Plasticity in Structural Material

S. R. Sabbagh-Yazdi, H. Najar-Nobari*

Department of Civil Engineering, KNToosi University of Technology, Tehran, Iran

P A P E R I N F O

Paper history:
Received 22 October 2019
Received in revised form 09 December 2019
Accepted 17 January 2020

Keywords:
Iterative Global/Local Method
Matrix-Free Galerkin Finite Volume Method
Non-intrusive Coupling
Nonlinear Element-Free Galerkin
Overlapping Multi-grid Patch

A B S T R A C T

This paper introduces a computational strategy to collaboratively develop the Galerkin Finite Volume Method (GFVM) as one of the most straightforward and efficient explicit numerical methods to solve structural problems encountering material nonlinearity in a small limited area, while the remainder of the domain represents a linear elastic behavior. In this regard, the Element Free Galerkin method (EFG), which is remarkably robust and accurate, but presumably more expensive, has locally been employed as a nonlinear sub-model to cover the shortcomings of the GFVM in the elastoplastic analysis. Since the formulations of these two methods are fundamentally different, the iterative zonal coupling has been accomplished using overlapping Multi-Grid (MG) patches with a non-matching interface and Iterative Global/Local (IGL) approach. The main property of such an algorithm is its non-intrusiveness, which means the complex nonlinear EFG solver is locally utilized over an elastic global GFVM without any geometric modification. This method is verified and investigated with available analytical and numerical solutions which gave quiet promising results showing the robustness and accuracy of the method. The Moving Least-Square approximation (MLS) has widely been applied on transfer level due to the non-conforming interface at the patch edges, and easily allows us to attach complex geometries with different mesh patterns. The new type of Quasi-Newtonian accelerator is adopted on the global material constitutive matrices and its convergence property and accuracy is compared with dynamic Aitken accelerators for two-dimensional problems in MATLAB. Finally, various accelerator types and mapping strategies are also concerned in the examination.

doi:*10.5829/ije.2020.33.03c.03*

NOMENCLATURE

C_{wave}	wave velocity	u^L, u^G	local and global displacement values
r_n	average size of equivalent control volume	σ^L, σ^G	local and global stress values
Ω^G, Ω^L	global and local domain	$F_{G\|L}$, $u_{G\|L}$	interfacial nodal forces and displacements
$\Omega^{G\|L}$	intersection of global and local domain	P, R	prolongation and restriction operators
D_{ep}	elasto-plastic material constitutive matrix	$\mu_{(k)}$	relaxation coefficient in the k_{th} step
d_{max}	dimensionless size of the support domain	K_L	local stiffness matrix
n_l, n_g	unit outward normal vector	Res^k	the interfacial residual L2-norm error

1. INTRODUCTION

In the numerical simulation of the material nonlinearity in large complex domains encountering small critical zones, it is very usual to implement a Finite Element (FE) solver on the entire domain. According to the established procedures, the nonlinear equilibrium equations are solved by dividing the external load into individual load increments and using Newton's method at each increment. These procedures could lead to unaffordable

*Corresponding Author Email: *h.nobari@mail.kntu.ac.ir* (H. Najar-Nobari)

Please cite this article as: S. R. Sabbagh-Yazdi, H. Najar-Nobari, Coupling Nonlinear Element Free Galerkin and Linear Galerkin Finite Volume Solver for 2D Modeling of Local Plasticity in Structural Material, International Journal of Engineering (IJE), IJE TRANSACTIONS C: Aspects Vol. 33, No. 3, (March 2020) 387-400

calculation costs, particularly in extremely large domains or complex load patterns. One of the drawbacks of such single-models, which have been widely used in computational mechanics, is that the overall efficiency is intensively influenced by the small nonlinear zones.

Multi-model approaches would be an appropriate answer to these limitations. The first choice is sub-modeling in which a global linear solver followed by a local nonlinear "patch" which covered the demanding global zone and operated by the global displacements [1], [2] or stresses [3]. In this regard, multiple specific methods can separately be employed in their relevant part. Although practically acceptable and analytically accurate, those methods suffer from a series of limitations such as a one-way data transition which neglects the global influence of local plasticity [4]. Therefore, stress redistribution and displacement compatibility, cannot be globally obtained. In this regard, some researchers have recommended a global iterative correction [5, 6], or static condensation [7, 8] to modify global results. Nevertheless, most of those were introduced as structural zooming or mesh adaptation just for linear elasticity, and are not entirely applicable for nonlinear analysis.

Another alternative is to employ multi-scale techniques [9] such as the micro/macro strategy [10], [11] or nonlinear localization techniques [12, 13]. Also the coupling techniques such as Implicit Direct Coupling Approach (IDCA) [14, 15],and Explicit Iterative Coupling Approach (EICA) [16] are the choice. In EICA solver, known as Neumann-Dirichlet, the required matrix dimension to solve the problem is much smaller than that of the conventional direct coupling. Whitcomb [6, 17] proposed The Iterative Global/Local (IGL) scheme based on EICA and noticed the severe converge problem to satisfy the equilibrium equation between the overlapping local grids and global background domain. In this regard, Carlos and Felippa [18] use Lagrange multipliers to satisfy the interface displacement compatibility, and various relaxation parameters were represented by Elleithy on transfer region to enhance the convergence level [19, 20]. In fact, those methods are robust and efficient, but they use complicated formulations which intrusively affect the global framework and therefore, commercial FE software or industrial data sets cannot be employed arbitrarily [21]. Although those techniques have proved their promising performance, it would be time-consuming and challenging to perform them in industrial applications. Consequently, they would be considered as a moderate solution, rather than an efficient practical technique. Recently, a non-intrusive IGL has been implemented by Duval and Passieux [22-27] to overcome the drawbacks by entirely releasing the global configuration. In this method, the global and local methods may include various geometric configurations, different mesh details, or independent governing constitutive laws. They can also be a separate piece of code, without any similarity. In spite of those efforts, the computational efficiency of such strategies is still an open issue and needs more discussion.

In this paper, we have developed a zonal coupling to improve the linear-elastic Galerkin Finite Volume solver (GFVM) [28, 29] by nesting the nonlinear Element Free Galerkin (EFG) [30, 31] to consider the local plasticity in structural material. The method is built on the non-intrusive IGL and some improvements are introduced that significantly enhance the accuracy and robustness of the method. The authors are globally utilized the GFVM, which is relatively efficient, accurate, and fast in terms of linear elasticity, to explicitly solve the problem and considerably simplify the modeling. Although the GFVM has proven to be effective in crack analysis [32], it is not preferable in terms of nonlinear analysis. Therefore, the EFG, which is more robust and mature technique, is patched with non-matching (nested) interface, to easily carry out the effects of local nonlinearity without suffering from heavy computational workload. The focus of the current study is to examine the feasibility of the explicit coupling for elastoplastic materials and the convergence of the proposed algorithm. Therefore, relatively simple elastoplastic problems with known analytical or finite element results are used for comparison to test the accuracy and efficiency of the proposed elastoplastic zonal coupling.

This method has some advantages, such as simpler formulae and directly transferring the interfacial boundary values. Altogether, the results of three numerical examples show that the computational speed and precision of the coupled method are higher than that of the single nonlinear EFG model.

In the present work, we extend the Quasi-Newtonian SR1 accelerator based on the material constitutive matrices to elastoplasticity. By means of this specific type of relaxation parameter, the iterative coupling between explicit and implicit solvers is easily become possible. The governing equation is obtained from the weak form of elastoplasticity over a local sub-domain, and the MLS approximation is used for data transferring on non-matching interfaces. The constitutive law is the small deformation, based on von Mises yielding criterion and strain general isotropic hardening.

2. GALERKIN FINITE VOLUME (GFVM) ON GLOBAL ELASTIC DOMAIN

GFVM is a precise, fast, and reliable numerical technique to solve boundary value problems, without any matrix operation, which was first introduced as a structural solver module of NASIR (Numerical Analyzer for Scientific and Industrial Requirements) software developed by Sabbagh-Yazdi et al. [32-35]. GFVM is an

iterative cell-vertex finite volume solver which solves the integral form of the governing equations on unstructured triangular meshes. This method is well-examined in various small strain mechanical problems as well as dynamic analysis [36], crack growth [37], dynamical failure [38, 39], and thermal elasticity [40].

According to this method, by multiplying the weight function (ω) by the Cauchy equation [33, 40], the Galerkin weak form is obtained as:

$$\int_{\Omega} \omega.\rho \frac{\partial^2 u_i}{\partial t^2} d\Omega = \int_{\Omega} \omega.\left(\vec{\nabla}.\vec{F_i}\right) d\Omega + \int_{\Omega} \omega.b_i \, d\Omega \quad (1)$$

where b is the body force, ρ the material mass density and F_i the force vector. By step-by-step integrating the first term on the right-hand side of the Equation (1), it could be rewritten as:

$$\int_{\Omega} \omega.\left(\vec{\nabla}.\vec{F_i}\right) d\Omega = \left[\omega.\vec{F_i}\right]_{\Gamma} - \int_{\Omega} \left(\vec{F_i}.\vec{\nabla}\omega\right) d\Omega \quad (2)$$

In Equation (2), while the weight function (ω) is equal to the linear interpolation function (ϕ), $[\omega.\vec{F_i}]_{\Gamma}$ would be zero on the boundaries of the integration subdomain. The last term of the Equation (1) is discretized as follows:

$$\begin{aligned} &-\int_{\Omega} \left(\vec{F_i}.\vec{\nabla}\omega\right) d\Omega \approx -\tfrac{1}{2}\textstyle\sum_{k=1}^{N}\left(\vec{\tilde{F}}_i\vec{\Delta l}\right)_k \\ &= \textstyle\sum_{k=1}^{N}(\tilde{\boldsymbol{\sigma}}_{i1}\Delta x_2 - \tilde{\boldsymbol{\sigma}}_{i2}\Delta x_1)_k \end{aligned} \quad (3)$$

In which $\vec{\Delta}\mathrm{l}_{\mathrm{k}}$ is the normal vector of the k_{th} surface. By applying the FDM concept to discretize the transient term of the Cauchy Equation by the algorithm mentioned by Sabbagh-Yazdi et al. [40] and by putting Equations (2) and (3) into (1), we finally have:

$$\begin{aligned} &(u_i)_n{}^{t+\Delta t} = 2(u_i)_n{}^{t} - (u_i)_n{}^{t-\Delta t} + \\ &\tfrac{3(\Delta t_n)^2}{2\rho\Omega_n}\left[\textstyle\sum_{k=1}^{N}(\tilde{\sigma}_{i1}\Delta x_2 - \tilde{\sigma}_{i2}\Delta x_1 + F_i)_k + \tfrac{2b_i\Omega_n}{3}\right]^t \end{aligned} \quad (4)$$

$$\begin{aligned} &\sigma_{ij} = \boldsymbol{C}u_{i,j} \approx \\ &\tfrac{1}{A_k}\textstyle\sum_{m=1}^{3} C\{u_x\Delta y \quad -u_y\Delta x \quad (u_x\Delta y - u_y\Delta x)\}_m \end{aligned} \quad (5)$$

where A_k is the area of the triangular element associated with the boundary k, and tensions are calculated at the center of the triangular element. Note that the time interval Δt_n does not have any physical interpretation in solving equilibrium problems and is only a virtual parameter used to solve the problem in an iterative manner [28]. The above explicit formulation requires an iterative process that converges during the progressive incremental procedure. In order to stabilize the explicit solution and to increase the convergence speed, appropriate time increment should be considered which depends on the material type and the control volume size which should be checked by Equation (6) for each control volume as follow:

$$\Delta t_n \leq \frac{r_n}{C_{wave}} \quad (6)$$

where C_{wave} is the wave velocity and r_n the average radius of equivalent circle that matches with the desired control volume [32].

3. NONLINEAR ELEMENT FREE GALERKIN (NL-EFG) ON LOCAL DOMAIN

For an elastoplastic state, the material stiffness continuously varies, and the incremental stress-strain relationship for each node is given by [41]:

$$d\sigma = \mathbf{D}_{ep} d\varepsilon \quad (7)$$

where $\mathbf{D}_{ep}$ is the elastoplastic material constitutive matrix, and $d\varepsilon$ the overall strain increment as follows:

$$d\varepsilon = d\varepsilon_e + d\varepsilon_p \quad (8)$$

where $d\varepsilon_e$ and $d\varepsilon_p$ are elastic and plastic strain increments. According to the Associated Flow Rule, the failure criterion is $f(\sigma) = 0$, where f is a failure function. According to the von Mises yield criterion, $f(\bar{\sigma}) = \bar{\sigma}^2/3$, where $\bar{\sigma}$ is the tensile yield stress. Having taken the derivatives, we obtain:

$$df = \frac{\partial f}{\partial \sigma} d\sigma + \frac{\partial f}{\partial \varepsilon_p} d\varepsilon_p = 0 \quad (9)$$

For simplicity, taking $\frac{\partial \mathrm{f}}{\partial \sigma} = \mathbf{a}^{\mathrm{T}}$ and $\mathbf{A} = -\frac{\partial f}{\partial \varepsilon_p}\mathbf{a}$, we can rewrite Equation (9) in the following form:

$$D_{ep} = D_e - \frac{D_e a a^T D_e}{[A + a^T D_e a]} \quad (10)$$

4. ITERATIVE OVERLAPPING COUPLING

Coupling (mixed) methods are classified as applied multi-model answers to overcome some of the limitations of single-model approaches. These techniques cover a wide range of multi-scale and multi-model approaches such as iterative coupling based on the Domain Decomposition (DD), direct coupling, multi-grid method, and IGLs. Each coupling method contains at least two separate systems of equations and corresponding results should be matched together on their boundary interfaces. It is quite crucial to mention that the main challenge, especially in the iterative schemes, is the convergence issue, and various alternatives have been proposed by several authors to overcome this issue.

In this paper, the GFVM was performed globally mainly due to its prominent speed and acceptable accuracy in linear parts of structural problems. Although GFVM is a vertex-based method which utilizes the Galerkin weighted residuals and linear shape functions for triangular elements, the final formulations were

obtained without any shape function; therefore, it is classified as an explicit solution. In other words, the whole problem would be solved locally without any global matrix. For the part of the problems with nonlinear behavior, we need a more efficient method rather than GFVM, and it could be any of the well-known precise non-linear methods. Therefore, EFG was chosen to solve local nonlinearities.

According to the fundamental differences between GFVM and EFG, the direct coupling of these two is not practically possible. Therefore the only choice is IGL and the best one would be the non-intrusive approach which has been implemented by Duval and Passieux [22-27]. One of the prominent advantages of the non-intrusive IGL is the integrity of the background mesh all over the solution processes. Therefore, the computational mesh outlasted completely intact during solution steps, which means the position and the number of nodes and elements always remain constant. Whereas many parameters are related to the nodal positioning and element geometries, most of the parameters such as tangential and orthogonal components of unit vectors, and the nodal and elemental surface area are calculated only once at the beginning of the solution. Altogether, the advantages of the non-intrusive IGL are outlined as follows:

- The background (global) mesh remains unchanged, which is especially valuable for cases where the global grid relates to a large-scale structure within a very large number of degree of freedom. Due to the reduction in the iterative computations caused by the generated grid, the stiffness matrix, force vectors and other global parameters were calculated once in the initialization of the computation.
- With the material non-linearity or crack discontinuity, a local grid can be created for complex non-linear analysis, which could be overlapped on the global grid.
- The local grid can be fully independent of the global background mesh. According to Figure 1, it can be observed that the local solution method can be different from the global model, in terms of the nodal distribution, density, layout, element degree of precision, and discretization techniques.
- The local model is represented as a corrector operator to improve the background results. Therefore, any model with specific characteristics can be applied for the non-linear area. As a consequence, a wide range of implicit and explicit numerical methods can be combined to increase the efficiency of the solution considering desired mechanical issues such as interaction, multi-scale, multi-grid, and coupling problems.

In terms of local and global positioning, coupled methods are divided into overlapping and non-overlapping systems. In non-overlapping system, the global configuration and parameters should fundamentally change according to the solution results of the plastic zone. Such a strategy not only is in conflict with the non-intrusiveness but also would end up with a significant convergence dilemma. In overlapping concept, various scenarios can be considered, for the local and global pattern. The simplest one is to utilize a part of the background nodes as common global/local nodes. The number and position of these nodes exactly match with the corresponding global nodes. Therefore, the data transition between these overlapped areas is accurately attainable at common nodes without any specific operator. Since we need more level of complexity and accuracy in the nonlinear analysis at the limited area, enough nodal density and accuracy, would not be provided by the same nodal configuration. Therefore, as illustrated in Figure 1, the non-matching form, in which the interfacial nodes are not necessarily compatible together, could be a feasible strategy.

4. 1. IGL Zonal Patching Formulation The global/local technique, divides the material nonlinear analysis into two parts:

(1) Linear elastic analysis of the global materials

(2) The local nonlinear analysis to consider failure and fracture criteria

In this regard, the force equilibrium and the displacement compatibility to pair Ω^L and Ω^G, are given as follows:

$$u = \begin{cases} u^{\text{Local}} & \text{in nonlinear area only} \\ u^{\text{Global}} & \text{everywhere else} \end{cases}$$
$$u^L = u^G \qquad \text{on } \Gamma \tag{11}$$
$$\sigma^L n_l + \sigma^G n_g = 0 \qquad \text{on } \Gamma$$

u^L, u^G, σ^L and σ^G are the interfacial values of displacements and stresses on the transition region between global and local areas. $\Omega^{G|L}$ is a part of the global domain, which overlaps with Ω^L, and Γ is the local boundary. Also, n_l and n_g are normal boundary vectors on local and global boundary nodes. Based on the non-intrusive framework, the solution algorithm contains only subdomain outputs, and the ultimate solution consists of neither a direct matrix relationship nor a combination of system matrices between different methods. In this regard, a special algorithm similar to the Newton-Raphson method may be used as follows [26]:

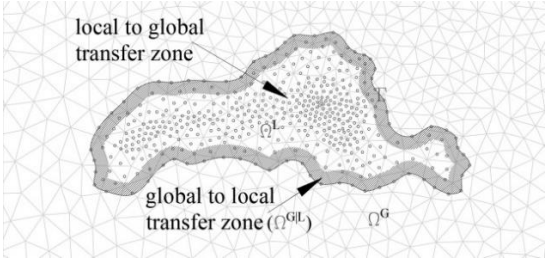

Figure 1. Non-matching configuration of the IGL and interface boundary edges

1. Global initial solution: Solve the problem assuming the entire domain is in the elastic condition.
2. Solution on local domain: The problem is solved locally affected by the parts of the global responses as boundary conditions. Although these boundary values can be nodal displacements or forces, the displacement integrity and compatibility would be guaranteed by displacement transition to the local edges.
3. Calculation of the residual values: Convergence is fundamentally dependent on the response equilibrium between two overlapping domains. In order to satisfy Equation (11) and reach convergence, the interfacial residual norm should be minimized.
4. Modification on the global material constitutive matrix and/or global stresses: If the residual norm of the displacements is not small enough, it will be added to the global domain as a correction value.

According to the above explanations, the correction of the global solution will appear in the following form [42]:

$$\mathbf{K}_G U_G^{k+1} = F_G^k + Res^k$$
$$Res^k = \left[\mathbf{K}_{G|L} U_G^k\right] - \left[R\mathbf{K}_L U_L^{k+\frac{1}{2}}\right] \quad (12)$$

where F_G^k and U_G^k are the global force and displacement vectors in step k_{th}, and R is the Restriction operator which maps local nodal values on global nodes. In this article, $(k-\frac{1}{2})$ always refers to local step between $(k-1)_{th}$ and $(k)_{th}$ global steps, and $(k+\frac{1}{2})$ refers to local step between $(k)_{th}$ and $(k+1)_{th}$ global steps. Multiplying $\mathbf{K}_G^{-1}$ by both sides of Equation (12), we get:

$$U_G^{k+1} = U_G^k + \mathbf{K}_G^{-1} Res^k \quad (13)$$

U_L in Equation (13) is defined as:

$$U_L^{k+\frac{1}{2}} = U_L^{k-\frac{1}{2}} + P\left[\Delta U_G^k\right]$$
$$\Delta U_G^k = U_G^{k-1} - R U_L^{k-\frac{1}{2}} = \mathbf{K}_G^{-1} Res^k \quad (14)$$

where P is the Prolongation operator to map global nodal values on local nodes. These interfacial values converge with regard to the following relationships and after several iterations (usually less than 5).

$$\mathbf{K}_L U_L^{k+1} = F_L \quad \text{with} \quad U_L^{k+1}\big|_\Gamma = P U_G^{k+1}\big|_\Gamma \quad (15)$$

These steps continue until Res^k or ΔU_G^{k+1} reduces to a predefined value. In Equation (15), $\mathbf{K}_L$ and $\mathbf{K}_G$ are the local and global stiffness matrices. In many cases, such as commercial software, it is almost impossible to extract the stiffness matrix. Moreover, in explicit solvers such as Matrix free GFVM, practically the stiffness matrix is meaningless. Here, based on the GFVM explicit solution in Equation (4), the displacements are the function of the last two sub-iterations as below:

$$u^{t+\Delta t} = \sum_{m=1}^{N} U\left(u^t \; u^{t-\Delta t} \; \sigma \; f \; b\right) \quad (16)$$

Then, according to the Hooke's law, Equation (13) can be modified as follow:

$$u_G^{k+1} = u_G^k + \sum_{m=1}^{N} U\left(\left\{u_G^k - \left[P^T u_L^{k+\frac{1}{2}}\right]\right\} \; \sigma_G \; f_G \; b_G\right) \quad (17)$$

If the local stresses are mapped onto the global domain as boundary tractions:

$$F_G^{k+1} = F_G^k + \sum_{m=1}^{N} F\left(u_G^t \left\{f_G^k - \left[P^T \mathbf{K}_L u_L^{k+\frac{1}{2}}\right]\right\} \; b_G\right) \quad (18)$$

In Equations (17) and (18), the local nonlinear EFG is implicitly solved as follow:

$$u_L^{k+\frac{1}{2}} = u_L^{k-\frac{1}{2}} + P\left[u_G^k - R u_L^{k-\frac{1}{2}}\right] \quad (19)$$

Multiplying $\mathbf{K}_L$ by both sides of Equation (19), we get the local force vector:

$$F_L^{k+\frac{1}{2}} = \mathbf{K}_L u_L^{k+\frac{1}{2}} = F_L^{k-\frac{1}{2}} + \left[\sigma_L^{k-\frac{1}{2}} - P\sigma_G^k\right]\Big|_{\Gamma^i}, \vec{n}_l^i \quad (20)$$

Equations (17) to (20) are the underlying framework of the proposed method. The convergence of these values will be obtained by Equation (15). Although these equations comprehensively represent the solution technique, since the non-linear computations never perform globally, the global stiffness would be more than the local one in the same area. Due to this inconsistency in the nonlinear zone, severe errors and instabilities would happen all over the solution domain. Disparity on stiffness amplitudes makes forces and displacements impossible to be concurrently balanced and practically complete convergence would never occur, and even after the convergence, the captured answer would not be valid. In this situation, to balance the forces and displacements, depending on which type of parameters transfer on transition zones, we encounter the following cases:

1. Sending (σ_G^k), and receiving $(u_L^{k+\frac{1}{2}})$ in return: in such circumstances, the global stresses (σ_G^k) are sent to local edges as a Neumann boundary traction, and in return, the local displacements $(u_L^{k+1/2})$ are received as a Dirichlet boundary condition on the global interface. The mentioned transformed boundary traction is equal to:

$$\Delta T_L^{k+\frac{1}{2}} = \tfrac{1}{2}\sum_{k=1}^{N}\left(\Delta\sigma_G^k, \vec{n}_l^i\right)_k$$
$$\Delta\sigma_G^k = \sigma_L^{k-\frac{1}{2}} - P\sigma_G^k \quad (21)$$

Here, the displacement compatibility would be automatically satisfied by enforcing the local nonlinear deformations on global interface. To control the force equilibrium, if $(\mathbf{D}_G^e)^{k+1}$ is updated according to the corresponding local values, the σ_G^{k+1} would be

automatically adjusted by each of the following equal terms:

$$\sigma_G^{k+1} = P^T \boldsymbol{\sigma}_L^{k+\frac{1}{2}} \tag{22}$$

$$\sigma_G^{k+1} = (\mathbf{D}_G^e)^{k+1} \varepsilon_G^{k+1} \tag{23}$$

Otherwise, if $(\mathbf{D}_G^e)^{k+1}$ is not modified, the results of Equation (23) will be much greater than Equation (22), because of the more global stiffness. Therefore, it is always preferred to update σ_G^{k+1} by Equation (22) at the end of the solution, to achieve the force equilibrium.

2. Sending (u_G^k), and receiving $(\boldsymbol{\sigma}_L^{k+1/2})$ in return: here, the global displacements (u_G^k) are sent to local edges as Dirichlet boundary condition, and the global stresses would be updated by the returned local stresses $(\boldsymbol{\sigma}_L^{k+1/2})$ at the end of each iteration. In this case, if $(\mathbf{D}_G^e)^{k+1}$ is modified according to the corresponding local values, (σ_G^{k+1}) would also be adjusted by Equations (22) or (23). Otherwise, due to the lack of returned displacement enforcement and differences between stiffnesses, the displacement compatibility would never be satisfied. Therefore, in return, not only the stresses but also the global material constitutive matrix should be updated by the local one. Meanwhile, to stabilize the static equilibrium, it is necessary to tie up at least two couples of neighbouring nodes.

3. Sending (u_G^k), and receiving $(u_L^{k+1/2})$ in return: in this case, the two-way displacement transition would guarantee solution convergence, but it is important to notice that the smaller the distance between these two transition areas, the higher the number of iterations. In fact, if these areas have any overlap, the results of the corresponding nodes would be exactly the same, which means that the solution will never converge.

4. Sending (σ_G^k), and receiving $(\boldsymbol{\sigma}_L^{k+1/2})$ in return: in this case, due to the lack of displacement consistency, the solution would be converged so hard; therefore, this approach will not be recommended.

In this paper, the first and second of the above cases are considered based on the following iterative algorithm which visualized in Figure 2.

4. 2. Convergence Algorithm Using Iterative Neumann-Dirichlet [19]

- Step 1: Solving the global problem disregarding any local effect and obtaining $\{u_G^0\}$ and $\{\sigma_G^0\}$ values.
- Step 2: Calculation of stresses $\{\sigma_G^k\}$ and displacements $\{u_G^k\}$ on global domain from Equations (4) and (5), at the beginning of each iteration ($k = 1,2, \ldots$).
- Step 3: Mapping global stresses $\{\sigma_G^k\}$ or global displacements $\{u_G^k\}$ on the local transition boundary as a traction $F_L^{k+1/2}$ or as an essential boundary condition $u_L^{k+1/2}$ based on the Equations (19) and (20) as follows:

$$u_L^{k+\frac{1}{2}}\Big|_{\Gamma^i} = u_L^{k-\frac{1}{2}}\Big|_{\Gamma^i} + P\Delta u_G^k\big|_{\Gamma^i} \tag{24}$$

$$F_L^{k+\frac{1}{2}}\Big|_{\Gamma^i} = \mathbf{K}_L u_L^{k-\frac{1}{2}} + \left[\boldsymbol{\sigma}_L^{k-\frac{1}{2}} - P\sigma_G^k\right]\Big|_{\Gamma^i}, \vec{n}_l^i \tag{25}$$

- Step 4: Computing $\boldsymbol{\sigma}_L^{k+\frac{1}{2}}$ and $u_L^{k+\frac{1}{2}}$ values and interpolating them on global interfacial nodes as $\{F_{G|L}^{k+1}\}$ or $\{u_{G|L}^{k+1}\}$ as follows:

$$\{u_{G|L}^{k+1}\} = u_G^{k+1}\big|_{\Gamma^i} = (1-\alpha)\, P^T, u_L^{k+\frac{1}{2}}\Big|_{\Gamma^i} + \alpha u_G^k\big|_{\Gamma^i} \tag{26}$$

$$\{F_{G|L}^{k+1}\} = F_G^{k+1}\big|_{\Gamma^i} = (1-\beta)P^T, \sigma_L^{k+\frac{1}{2}}, \vec{n}_j^{iG} + \beta F_G^k\big|_{\Gamma^i} \tag{27}$$

where α and β are relaxation parameters to accelerate and guarantee the convergence, which will be presented, in more details, in section 0.

- Step 5: Modifying global displacements $\{u_G^{k+1}\}$ or $\{\sigma_G^{k+1}\}$ at local boundary for next computational step according to the Equations (17) and (18) using the last accelerated boundary values.
- Step 6: Convergence control:

$$\text{if} \begin{cases} \frac{\|u_G^{k+1} - u_G^k\|}{\|u_G^{k+1}\|} < \varepsilon \\ \frac{\|F_G^{k+1} - F_G^k\|}{\|F_G^{k+1}\|} < \varepsilon \end{cases} : \{\text{stop}\} \quad \text{else: } \{k \to k+1\} \tag{28}$$

In the above algorithm, steps 2-5 are called multi-grid cycles.

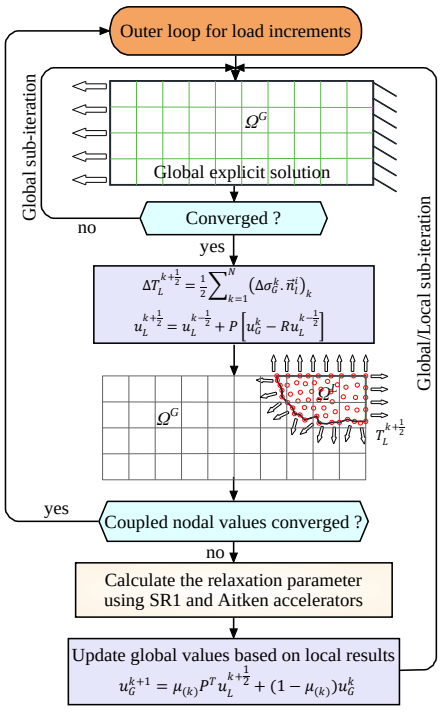

Figure 2. Flowchart for nonlinear zonal coupling

4. 3. Convergence, Relaxation Parameters, and Accelerators The most critical point in iterative coupling is the convergence, which depends on the differences in tensions, deformations and mechanical properties of the materials on two overlapping areas and their boundaries. Figure 3 illustrates the linear oscillation of the global/local edges in order to match together. To accelerate the convergence speed, and smoothen the oscillations, some relaxation parameters should be implemented. One of these acceleration techniques is the quasi-Newtonian family in which the Symmetric Rank One (SR1) formula was employed to accelerate the convergence rate by Gendre et al. [26]. Although it enhances the convergence speed, the updating process of the global stiffness is complicated.

Another acceleration technique that modifies interface parameters without updating the global stiffness matrix is Aitken's Δ^2 accelerator [43]. This method is one of the most effective accelerators which linearly converge and relax the iterative processes as follow:

$$u_G^{k+1} = \mu_{(k)} P^T u_L^{k+\frac{1}{2}} + (1-\mu_{(k)}) u_G^k \tag{29}$$

where $\mu_{(k)}$ is the relaxation coefficient in the k_{th} step obtained from the results of the two previous steps, u_G^{k+1} is the displacement value used in the next global step and $P^T u_L^{k+1/2}$ is the processed local displacement at the end of k_{th} step. In order to estimate the optimum relaxation factor, the following functional is considered [16]:

$$f(\lambda) = \left\| u_G^{k+1} - u_G^k \right\|^2 \tag{30}$$

By putting Equation (29) in Equation (30), we have:

$$f(\mu_{(k)}) = \left\| \mu_{(k)} \left\{ P^T u_L^{k+\frac{1}{2}} - P^T u_L^{k-\frac{1}{2}} \right\} + (1-\mu_{(k)}) \{ u_G^k - u_G^{k-1} \} \right\|^2 \tag{31}$$

To achieve the optimum value for $\mu_{(k)}$, one should compute the extremum of Equation (31) by deriving from this parameter. If we assume $P^T u_L^{k+1/2} - P^T u_L^{k-1/2} = \Delta\left(P^T u_L^{k+1/2}\right)$ and $u_G^k - u_G^{k-1} = \Delta u_G^k$, then by sorting the equation, the value of $\mu_{(k)}$ is obtained as follow:

$$\frac{\partial f(\mu_{(k)})}{\partial \mu_{(k)}} = 2 \left\| \mu_{(k)} \Delta\left(P^T u_L^{k+\frac{1}{2}} \right) + (1-\mu_{(k)}) \Delta u_G^k \right\| \left\| \Delta\left(P^T u_L^{k+\frac{1}{2}} \right) - \Delta u_G^k \right\| = 0$$

$$\Rightarrow \mu_{(k+1)} = -\mu_{(k)} \frac{\left(\Delta u_G^k, \left(\Delta u_G^k - \Delta\left(P^T u_L^{k+\frac{1}{2}} \right) \right) \right)}{\left\| \Delta u_G^k - \Delta\left(P^T u_L^{k+\frac{1}{2}} \right) \right\|^2} \tag{32}$$

The relaxation coefficient obtained from Equation (32) must be calculated and used for each step between two individual domains. For the first two iterations, $\mu_{(k)}$ is assumed to be equal to one, i.e. $u_G^0 = P^T u_L^0$ and $u_G^1 = P^T u_L^1$. It is also possible to use this coefficient by replacing the stress instead of the displacement in order to modify the global stresses as follows:

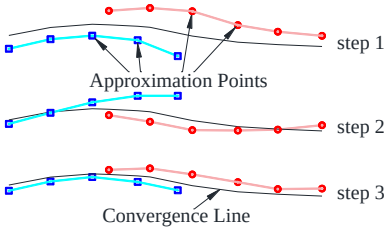

Figure 3. 1D representation of convergence concept in global/local method at the interface boundary

$$\sigma_G^{k+1} = \mu_{(k)} P^T \boldsymbol{\sigma}_L^{k+\frac{1}{2}} + (1-\mu_{(k)}) \sigma_G^k \tag{33}$$

Also, to modify the global material matrix we have:

$$\mathbf{D}_G^{k+1}(x) = \mu_{(k)} P^T \mathbf{D}_L^{k+\frac{1}{2}}(x) + (1-\mu_{(k)}) \mathbf{D}_G^k(x) \tag{34}$$

Another way to accelerate the convergence is to use Quasi-Newtonian methods to update the stiffness matrix. If $\Delta u_G^k = u_G^{k+1} - u_G^k$ and $\Delta f_G^k = f_G^{k+1} - f_G^k$, then by SR1 and secant equations, $\mathbf{K}_G^{k+1}$ would be calculated as follows [23], [26]:

$$\mathbf{K}_G^{k+1} = \mathbf{K}_G^k + \frac{(\Delta f_G^k - \mathbf{K}_G^k \Delta u_G^k)(\Delta f_G^k - \mathbf{K}_G^k \Delta u_G^k)^T}{(\Delta u_G^k)^T (\Delta f_G^k - \mathbf{K}_G^k \Delta u_G^k)} \cong \mathbf{K}_G^k + \frac{(f_G^{k+1})(f_G^{k+1})^T}{(\Delta u_G^k)^T (f_G^{k+1})} \tag{35}$$

As noted above, in many cases, access to the stiffness matrix is not possible, or the method is fundamentally matrix-free. In GFVM, the only parameter between stress and strain values is the material constitutive matrix, and here we can use Equation (35) to update this matrix instead of the stiffness matrix.

$$\mathbf{D}_G^{k+1} = \mathbf{D}_G^k + \frac{(\Delta \sigma_G^k - \mathbf{D}_G^k \Delta \varepsilon_G^k)(\Delta \sigma_G^k - \mathbf{D}_G^k \Delta \varepsilon_G^k)^T}{(\Delta \varepsilon_G^k)^T (\Delta \sigma_G^k - \mathbf{D}_G^k \Delta \varepsilon_G^k)} \cong \mathbf{D}_G^k + \frac{(\sigma_G^{k+1})(\sigma_G^{k+1})^T}{(\Delta \varepsilon_G^k)^T (\sigma_G^{k+1})} \tag{36}$$

The $\mathbf{D}_G^{k+1}$ obtained from Equations (34) or (36) could be implemented to compute global stress and displacement based on Hooke's law on $(k+1)_{th}$ step. The total error at each iteration is estimated by L2-norm based on Equation (37). The iteration should be continued until this value is reduced by $\varepsilon = 10^{-5}$.

$$Tol = \frac{Sqrt\left\{ \sum_{j=1}^{N} \left\{ \left(U_x^{\langle j \rangle}\Big|^{GFVM} - U_x^{\langle j \rangle}\Big|^{EFG} \right)^2 + \left(U_y^{\langle j \rangle}\Big|^{GFVM} - U_y^{\langle j \rangle}\Big|^{EFG} \right)^2 \right\} \right\}}{Sqrt\left\{ \sum_{j=1}^{N} \left\{ \left(U_x^{\langle j \rangle}\Big|^{GFVM} \right)^2 + \left(U_y^{\langle j \rangle}\Big|^{GFVM} \right)^2 \right\} \right\}} \times 100\% < \varepsilon \tag{37}$$

The proposed non-intrusive overlapping concepts can be categorized into four following different types as shown in Table 1.

5. NUMERICAL EXAMPLES

In this section, two numerical examples of two-dimensional elasto-plasticity problems are solved using the coupled GFVM-EFG method. The examples include the cantilever beam subjected to a concentrated load, and a finite plate with a hole. Results from the proposed method are verified with EFG and FEM results using commercial software ANSYS. Since EFG and FEM results are approximate solutions, very dense mesh density was implemented to regard these solutions as practically exact. These models are also used for comparison; therefore, care was taken to ensure that all nodes in a proposed model coincide exactly with a subset of nodes in the corresponding EFG or FEM model in order to facilitate direct comparison.

5. 1. A Cantilever Beam Subjected to a Concentrated Loading A plane stress cantilever beam subjected to a concentrated load applied monotonically in ten increments at the free end is considered. This case was previously examined by Cheng [44] and we compare our results to examine the validity of the solution. The length of the beam is L=8m, the height and width are 1m, and the concentrated load is F=1N (see Figure 4). The material modulus of elasticity is $E=10^5$Pa, the Poisson's ratio is ν=0.25 and the yielding stress is σ_y=25Pa. The von Mises yield criterion is used and the linear strain hardening modulus is equal to 20kPa. The global domain consists of 633 nodes and 1107 triangular elements. The maximum nodal distance of the local EFG domain is 2cm. The local EFG solver uses a circular zone as the support domain of each node, and the scaling parameter determining the size of the support domain is d_{max}=3. The initial local domain has 162 uniformly distributed nodes and it proportionally changed and increased at each load increment. The local domain boundary is set to be at least the 5 cm distance from the edges of the non-linear area.

TABLE 1. Non-intrusive classification based on the interface parameters

Method	Prolonged data	Restricted data
M_1(a), M_1(b)	Displacement	Constitutive matrix
M_2(a), M_2(b)	Traction	Displacement & Constitutive matrix

(a) Aitken's Δ^2, (b) Quasi-newton SR1

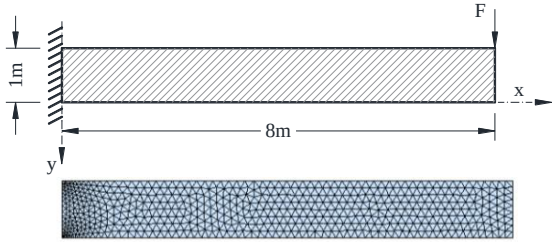

Figure 4. Cantilever beam subjected to a concentrated load

We use the coupled method presented in this paper to solve the global problem. Figure 5 shows the numerical solutions of the displacements u_y at y=0. It is shown that the numerical results of the proposed method are in excellent agreement with the ones obtained with the non-linear EFG and FE ANSYS software.

Figure 6 shows the load-displacement diagram of the midpoint at the left-end of the beam. The non-linear behavior of the beam can apparently be seen, and it is quite clear that the entire results have good agreement with the FEM results.

5. 2. Finite Plate with a Circular Hole The next numerical example is a plane stress finite plate with a circular hole in the center subjected to a uniform displacement in y direction at the top and bottom sides of the plate. This problem is well-known in academic literature, so our results and procedures would also be compared with Jianfeng [45] to examine the validity of the non-linear solution. For simplicity, only a quarter of the plate was modeled due to the symmetric condition, using proper boundary conditions (illustrated in Figure 7). The modeled part of the plate is 5m by 5m in which the part of the circular hole of 1m radius is located at the

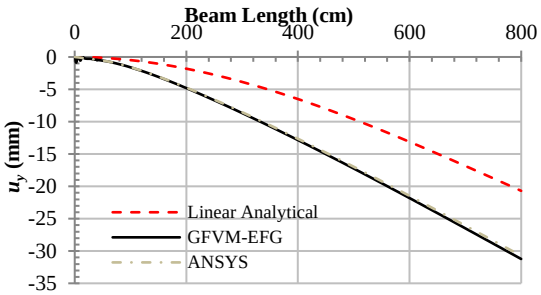

Figure 5. The u_y displacements at y=0

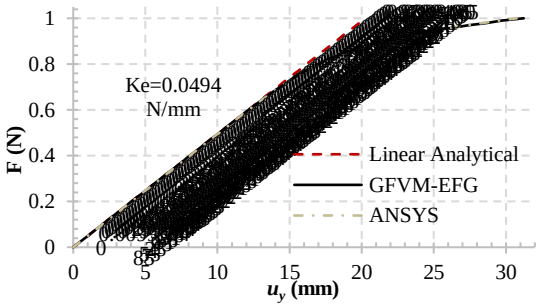

Figure 6. The cantilever load-displacement diagram at the end of the beam

lower left corner. The global model has 951 nodes and 1794 triangular elements (see Figure 11a1–c1). The maximum nodal distance in the local EFG domain is 5cm. The local EFG solver uses a circular zone as the support domain of each node, and the scaling parameter determining the size of the support domain is d_{max}=3. The material is ASTM A514 structural steel with Young's modulus of 2.1e5 MPa, Poisson's ratio of 0.3, yield stress of 900 MPa, and tangent modulus of 1000 MPa. All methods mentioned in Table 1 are considered in this example. To clarify the basic concept of the M_2 method, the transmitted global stresses over the local boundaries are illustrated in Figure 8 as boundary tractions.

The yielding initially occurs on the critical value of U_y equal to b=0.7672cm and at the edge of the circular hole. By increasing the computed value of U_y to 1.303b, 1.824b, and 2.346b, the L2-norm comparison between the entirely converged displacements of the proposed modeling strategy using various non-intrusive interfacing methods and ANSYS solution is represented in Table 2.

Figures 9 and 10 present the distribution of σ_{yy} and von Mises stress (σ_{VM}) along y=0, and the good agreement between proposed method and the ANSYS results is indicated. As can be seen, the maximum value of the σ_{yy}, as expected, is about 9000 kg/cm^2. The spreading of plastic zone for various amount of U_y is shown in Figure 11a–c. For each case, the local configuration and the plastic area are visualized and compared. The final local node numbers at the end of the solution, as illustrated in Figure 11a1–c1, are 180, 367, and 1284 for various U_y values. It is quite clear that the plastic area is intensively spread after its initiation.

TABLE 2. L2-norm errors in comparison with ANSYS

	Method	U_y=1.303b	1.824b	2.346b
Coupled EFG-GFVM	M_1	3.05e^{-5}	1.53e^{-4}	5.95e^{-4}
	M_1(a)	9.32e^{-6}	2.80e^{-5}	5.59e^{-5}
	M_1(b)	1.18e^{-5}	3.30e^{-5}	7.27e^{-5}
	M_2	1.13e^{-4}	1.08e^{-4}	2.20e^{-3}
	M_2(a)	7.50e^{-5}	2.03e^{-4}	5.67e^{-4}
	M_2(b)	8.10e^{-5}	2.51e^{-4}	8.04e^{-4}

To determine the efficiency of the proposed method, the comparison with Single-EFG-model with various node densities for Uy=2.346b=1.8cm is performed. The corresponding accuracy and CPU time for each method are represented in Table 3. We can see that at the same level of accuracy, the CPU time for single EFG model is 761 sec, which is 11% more than that of the proposed coupled M2(a) method (682 sec). However, more efficiency and accuracy may be achieved for GFVM-EFG model, if the more accurate non-intrusive interfacing method is applied. Therefore, it can be stated that the coupled one can improve the solution accuracy and efficiency compared to the traditional EFG method. The CPU time for M1(a) and M1(b) is 912 and 871 sec,

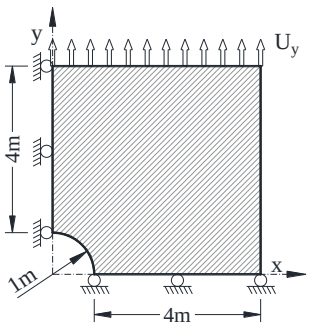

Figure 7. The upper right quadrant of the plate with a hole

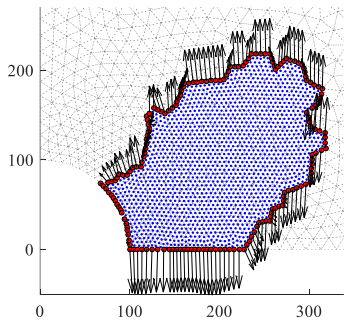

Figure 8. σ_{VM} on global deformed shape U_y =2.346b

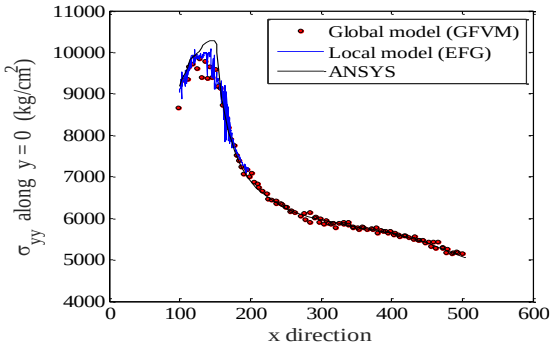

Figure 9. σyy along y=0 for Uy=824b

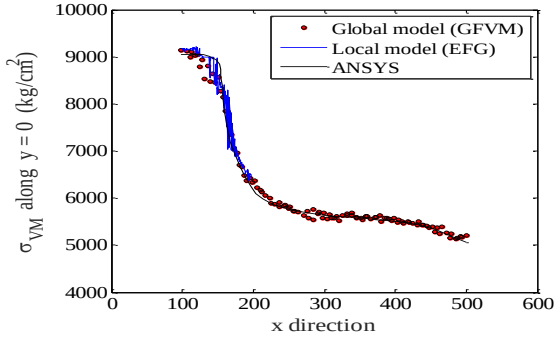

Figure 10. σ_{VM} along y=0 for Uy=824b

which is 33% and 27% more than M2(a) and M2(b). This is absolutely due to the more iteration in M1 than M2.

The σ_{VM} on deformed shape of the problem domain has been illustrated in Figure 12. Moreover, the σ_{VM} is separately presented for U_y =2.346b on local and global configuration in Figure 13. As can be seen, good agreement between overlapping local and global results is indicated. In these figures the displacements are multiplied by 100 for clarity.

To demonstrate the iterative behavior of the proposed method, the comparison between M_1 and M_2 models has been implemented and the results are respectively illustrated in Figure 14 and Figure 15. At each load step, Global/Local and Newton-Raphson (NR) iterations are performed individually until the decrease of L2-norm comes within 10^{-5}. In M_2 (Figure 15) convergence was obtained with less than 9 coupling iterations at maximum state, but in M_1 (Figure 14) the number of essential iterations is more than 9. In both of these figures, the overall errors seem to diverge, but in fact, the local area is continually getting larger and the corresponding initial error is increased.

Figure 16 shows the Newton-Raphson iteration numbers and their corresponding L2-Norm errors. As can be seen, both of these values intensively decrease after the first coupling iteration.

TABLE 3. The CPU time (sec) vs. accuracy in the last load increment

	Method	Number of nodes	Time (sec)	L2-norm
Coupled EFG-GFVM	M_1	(951 global nodes & 1284 local nodes)	2226	5.95e^{-4}
	M_1(a)		912	5.59e^{-5}
	M_1(b)		871	7.27e^{-5}
	M_2		1650	2.20e^{-3}
	M_2(a)		**682**	**5.67e^{-4}**
	M_2(b)		690	8.04e^{-4}
Single-EFG-model		(415 nodes)	38	8.86e^{-3}
		(951 nodes)*	167	1.03e^{-3}
		(2913 nodes)	**761**	**5.80e^{-4}**
		(5141 nodes)	1975	1.17e^{-6}

* The same node distribution as global mesh

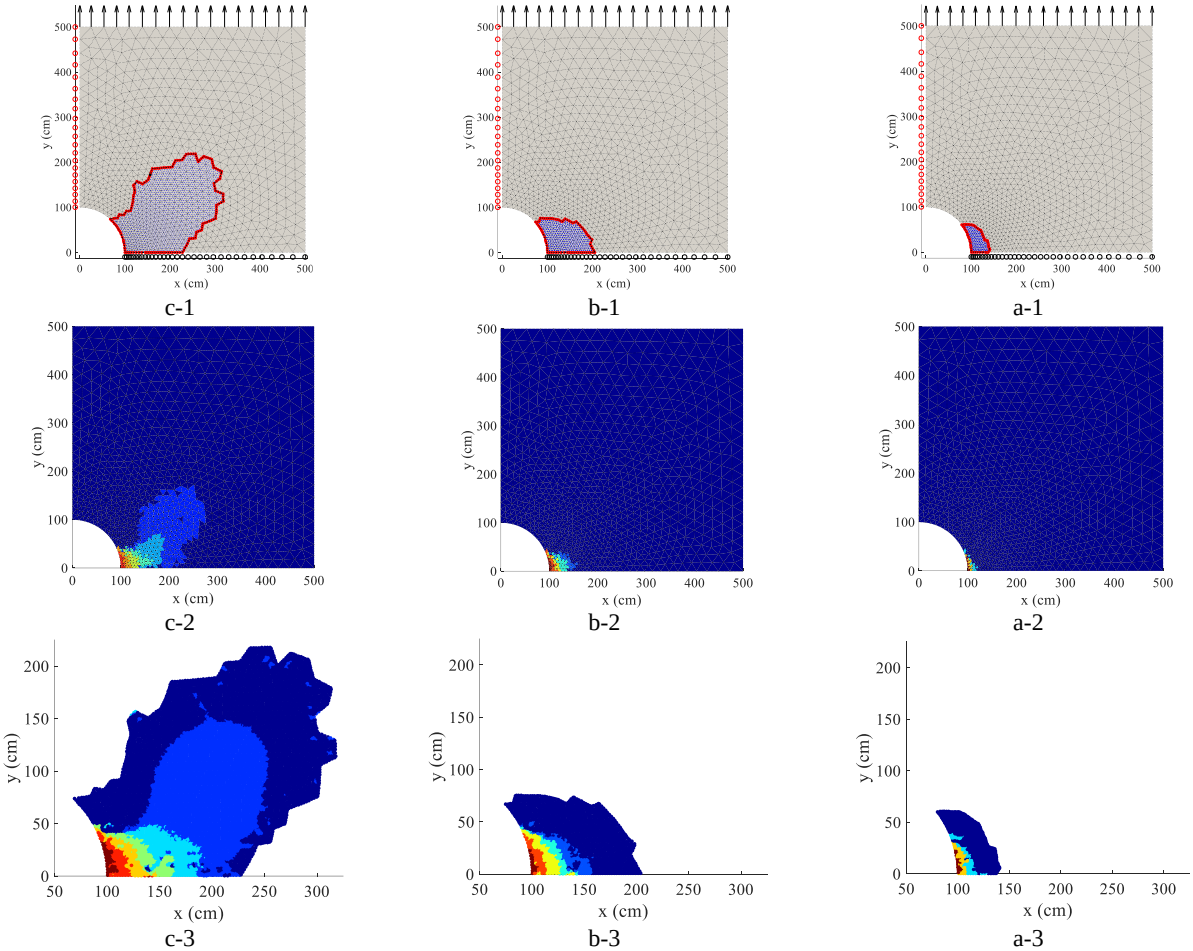

Figure 11. Spreading of plastic zone: a) $U_y = 1.303b$, b) $U_y = 1.824b$ c) $U_y = 2.346b$

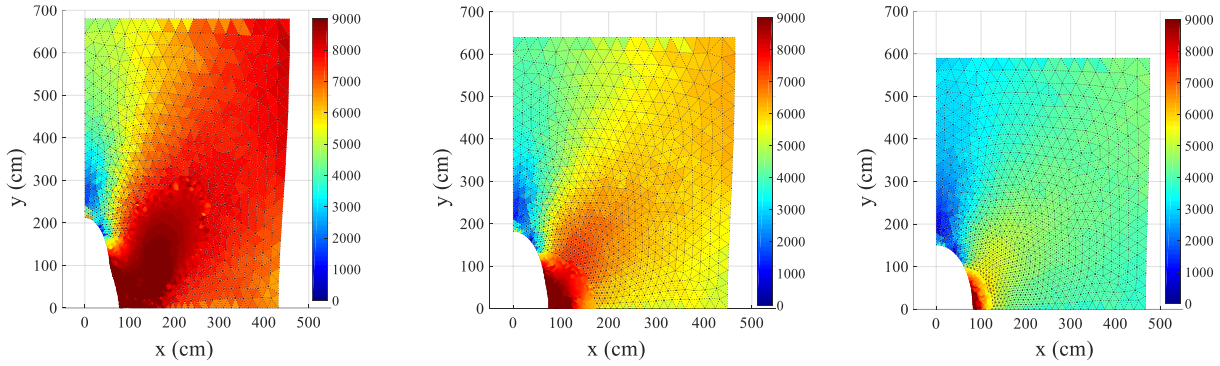

Figure 12. von Mises stress contour on the global and local domain for *Uy* being 1.303*b*, 1.824*b*, and 2.346*b* respectively

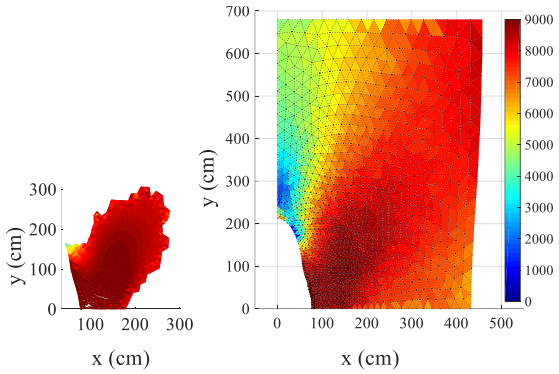

Figure 13. σ_{VM} on the global and local deformed shape respectively at U_y =2.346*b*

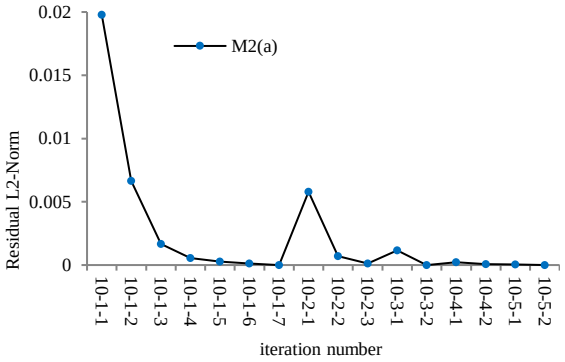

Figure 16. Newton-Raphson iterations through 5 coupling iterations in M_1(a)

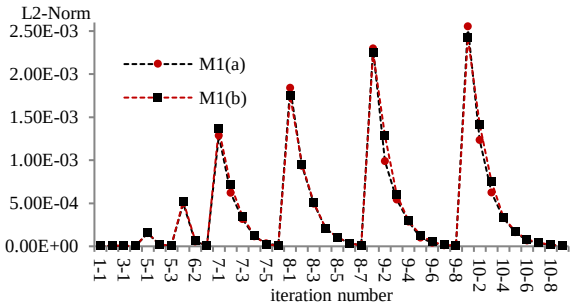

Figure 14. The convergence error at each iteration in M1(a) and M1(b)

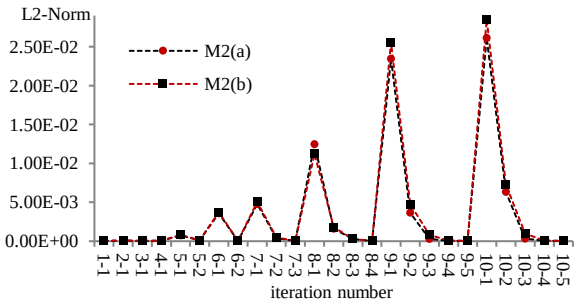

Figure 15. The convergence error at each iteration in M_2(a) and M_2(b)

6. CONCLUSION

In this paper, a non-intrusive IGL is presented to analyze linear structure with local nonlinearity. This algorithm extends the iterative global/local method to treat non-matching (incompatible) interface mesh. Since the algorithm is non-intrusive, it can be easily applied by various numerical techniques to the analysis of large-scale structure with local nonlinear phenomenon in engineering. In this regard, the GFVM and EFG methods are implemented respectively as global and local configuration due to their advantages.

Due to the non-conforming (nested) interface at the patch edge, the virtual interface is introduced to link the global coarse mesh and the local fine nodes, using the properties of MLS approximation to guarantee the reliability of the method.

Since the convergence rate is relatively slow, especially when the interface geometry is complicated, the simple and efficient acceleration techniques based on Aitken's Δ^2 and Quasi-Newtonian SR1 method are employed to improve the convergence property.

In order to verify the algorithm, numerical experiments are conducted on 2D model with local plasticity. The accuracy of this algorithm is validated by

comparing it with an approximate numerical reference FE model.

To summarize the achievements of coupling local Non-linear EFG and global linear GFVM Solvers for 2D modeling of local plasticity in structural material, the following main conclusions can be stated:

(1) The algorithm is very robust in non-matching interface data transfer, which can overcome the accumulation of the numerical error during iterative analyses. Thus, it is very efficient in numerical performance and can lead to a more general and wider application in local nonlinear analyses.

(2) Aitken's Δ^2 acceleration method is significantly efficient to speed up the convergence rate and improve the accuracy, especially for the complex interface geometry cases.

(3) Since the MLS-based data transfer scheme is very feasible to implement, the IGL algorithm is highly non-intrusive with the traditional FE environment to treat non-matching meshes. In consequence, this IGL method is very suitable to analyze large-scale structure with local nonlinearities in engineering.

The computational results demonstrated in this paper show that for the cases in which the nonlinear plastic zone may be limited to a small portion of the computational domain, coupling local nonlinear comparison with global linear GFVM (in conjunction with application of non-intrusive interface boundary data transmission) provides better efficiency and accuracy than using a nonlinear method (like EFG) for the entire domain. The proposed computational efficiency of the proposed method is promising for its application in time dependent (progressive) non-linear structural problems.

7. REFERENCES

1. Cormier, N.G., Smallwood, B.S., Sinclair, G.B. and Meda, G., "Aggressive submodelling of stress concentrations", ***International Journal for Numerical Methods in Engineering***, Vol. 46, No. 6, (1999), 889–909.
2. Kelley, C. T. and Sachs, E. W., "Local Convergence of the Symmetric Rank-One Iteration", ***Computational Optimization and Applications***, Vol. 9, No. 1, (1998), 43–63.
3. Jara-Almonte, C. C. and Knight, C. E., "The specified boundary stiffness/force SBSF method for finite element subregion analysis", ***International Journal for Numerical Methods in Engineering***, Vol. 26, No. 7, (1988), 1567–1578.
4. Emeka, A. E., Jonah Chukwuemeka, A., and Benjamin.Okwudili, M., "Deformation Behaviour of Erodible Soil Stabilized with Cement and Quarry Dust", ***Emerging Science Journal***, Vol. 2, No. 6, (2018), 383.
5. Mao, K. M. and Sun, C. T., "A refined global-local finite element analysis method", ***International Journal for Numerical Methods in Engineering***, Vol. 32, No. 1, (1991), 29–43.
6. Whitcomb, J. D., Iterative global/local finite element analysis", ***Computers and Structures***, Vol. 40, No. 4, (1991), 1027–1031.
7. Hirai, I., Wang, B. P., and Pilkey, W. D., "An efficient zooming method for finite element analysis", ***International Journal for Numerical Methods in Engineering***, Vol. 20, No. 9, (1984), 1671–1683.
8. Hirai, I., Uchiyama, Y., Mizuta, Y. and Pilkey, W.D., "An exact zooming method", ***Finite Elements in Analysis and Design***, Vol. 1, No. 1, (1985), 61–69.
9. Mandel, J. and Dohrmann, C. R., "Convergence of a balancing domain decomposition by constraints and energy minimization", ***Numerical Linear Algebra with Applications***, Vol. 10, No. 7, (2003), 639–659.
10. Ladevèze, P. and Dureisseix, D., "A micro / macro approach for parallel computing of heterogeneous structures", ***International Journal for Computational Civil and Structural Engineering***, Vol. 1, (2017), 180-28.
11. Naderi, A. and Baradaran, G. H., "Element free galerkin method for static analysis of thin micro/nanoscale plates based on the nonlocal plate theory", ***International Journal of Engineering, Transactions A: Basics***, Vol. 26, No. 7, (2013), 795–806.
12. Cresta, P., Allix, O., Rey, C. and Guinard, S., "Nonlinear localization strategies for domain decomposition methods: Application to post-buckling analyses", ***Computer Methods in Applied Mechanics and Engineering***, Vol. 196, No. 8, (2007), 1436–1446.
13. Bagheri, A., Baradaran, G.H. and Mahmoodabadi, M.J., "Meshless Local Petrov-galerkin Method for Elasto-static Analysis of Thick-walled Isotropic Laminated Cylinders", ***International Journal of Engineering - Transactions B: Applications***, Vol. 27, No. 11, (2014), 1731–1740.
14. Belytschko, T., Organ, D., and Krongauz, Y., "A coupled finite element-element-free Galerkin method", ***Computational Mechanics***, Vol. 17, No. 3, (1995), 186–195.
15. Aour, B., Rahmani, O., and Nait-Abdelaziz, M., "A coupled FEM/BEM approach and its accuracy for solving crack problems in fracture mechanics", ***International Journal of Solids and Structures***, Vol. 44, No. 7–8, (2007), 2523–2539.
16. Godinho, L., Soares Jr, D., Pereira, A. and Dors, C., "Iterative coupling between the MFS and Kansa's method for acoustic problems", ***WIT Transactions on Modelling and Simulation***, Vol. 54, (2013), 123–132.
17. Whitcomb, J. D. and Woo, K., "Application of Iterative Global/Local Finite Element Analysis. Part 1: Linear Analysis", ***Communications in Numerical Methods in Engineering***, Vol. 9, No. 9, (1993), 745–756.
18. Park, K. C., Felippa, C. A., and Rebel, G., "A simple algorithm for localized construction of non-matching structural interfaces", ***International Journal for Numerical Methods in Engineering***, Vol. 53, No. 9, (2002), 2117–2142.
19. El-Gebeily, M., Elleithy, W. M., and Al-Gahtani, H. J., "Convergence of the domain decomposition finite element-boundary element coupling methods", ***Computer Methods in Applied Mechanics and Engineering***, Vol. 191, No. 43, (2002), 4851–4867.
20. Elleithy, W. M., Tanaka, M., and Guzik, A., "Interface relaxation FEM-BEM coupling method for elasto-plastic analysis", ***Engineering Analysis with Boundary Elements***, Vol. 28, No. 7, (2004), 849–857.
21. Forcellini, D., Tanganelli, M., and Viti, S., "Response Site Analyses of 3D Homogeneous Soil Models", ***Emerging Science Journal***, Vol. 2, No. 5, (2018), 238.
22. Duval, M., Lozinski, A., Passieux, J.C. and Salaün, M., "Non-intrusive coupling : multiscale computation and finite element mesh adaptation", In eXtended Discretization MethodS (X-DMS 2015), Italy, (2015), 3–5.
23. Duval, M., Passieux, J.C., Salaün, M. and Guinard, S., "Non-intrusive Coupling: Recent Advances and Scalable Nonlinear Domain Decomposition", ***Archives of Computational Methods***

in Engineering, Vol. 23, No. 1, (2016), 17–38.

24. Duval, M., Guinard, S., Passieux, J.C. and Salaun, M., "Non-intrusive domain decomposition algorithm for solving nonlinear problems", In ECCOMAS Congress - European Congress on Computational Methods in Applied Sciences and Engineering, (2016).
25. Kerfriden, P., Passieux, J. C., and Bordas, S. P. A., "Local / global model order reduction strategy for the simulation of quasi-brittle fracture", ***International Journal for Numerical Methods in Engineering***, Vol. 89, No. 2, (2012), 154-179.
26. Allix, O., Gendre, L., Gosselet, P. and Guguin, G., Non-intrusive coupling: An attempt to merge industrial and research software capabilities", In Recent developments and innovative applications in computational mechanics, Springer, Heidelberg, (2011), 125-133.
27. Gendre, L., Allix, O., Gosselet, P. and Comte, F., "Non-intrusive and exact global/local techniques for structural problems with local plasticity", *Computational Mechanics*,Vol. 44, No. 2, (2009), 233–245.
28. Sabbagh-Yazdi, S. R., Ali-Mohammadi, S., and Pipelzadeh, M. K., "Unstructured finite volume method for matrix free explicit solution of stress-strain fields in two dimensional problems with curved boundaries in equilibrium condition", ***Applied Mathematical Modelling***, Vol. 36, No. 5, (2012), 2224–2236.
29. Yazdi, S. R. S., Amiri, T., and Gharebaghi, S. A., "A Proposed Damping Coefficient of Quick Adaptive Galerkin Finite Volume Solver for Elasticity Problems", ***Journal of the Serbian Society for Computational Mechanics***, Vol. 13, No. 1, (2019), 56–79.
30. Ghorashi, S. S., Sabbagh-Yazdi, S. R., and Mohammadi, S., "Element free Galerkin method for crack analysis of orthotropic plates", Computational Methods in Civil Engineering, Vol. 1, No. 1, (2010), 1–13.
31. Ahmed, M., Singh, D., and Desmukh, M. N., "Element Free Galerkin Post-processing Technique Based Error Estimator for Elasticity Problems", ***Civil Engineering Journal***, Vol. 4, No. 12, (2018), 2946-2958.
32. Sabbagh-Yazdi, S. R., Farhoud, A., and Asil Gharebaghi, S., "Simulation of 2D linear crack growth under constant load using GFVM and two-point displacement extrapolation method", ***Applied Mathematical Modelling***, Vol. 61, (2018), 650–667.
33. Sabbagh-Yazdi, S. R., Mastorakis, N. E., and Esmaili, M., "Explicit 2D Matrix Free Galerkin Finite Volume Solution of Plane Strain Structural Problems on Triangular Meshes", ***International Journal of Mathematics and Computers in Simulations***, Vol. 2, No. 1, (2008), 1–8.
34. Sabbagh-Yazdi, S. R., Amiri-SaadatAbadi, T., and Wegian, F. M., "2D Linear Galerkin finite volume analysis of thermal stresses during sequential layer settings of mass concrete considering contact interface and variations of material properties: Part 1: Thermal analysis", ***Journal of the South African Institution of Civil Engineering***, Vol. 55, No. 1, (2013), 94–103.
35. Alkhamis, M.T., Sabbagh-Yazdi, S.R., Esmaeili, M. and Wegian, F.M., "Utilizing NASIR galerkin finite volume analyzer for 2D plane strain problems under static and vibrating concentrated loads", ***Jordan Journal of Civil Engineering***, Vol. 2, No. 4, (2008), 335–343.
36. Sabbagh-Yazdi, S. R. and Bayatlou, M., "Application of Finite Volume Method for Structural Analysis", (2013), 1-7. http://khi.ac.ir/Research_Portal/5thsastech/Civil/Civil_39.pdf.
37. Sabbagh-Yazdi, S. R. and Bayatlou, M., "Equilibrium condition nonlinear modeling of a cracked concrete beam using a 2D Galerkin finite volume solver", ***Computational Methods in Civil Engineering***, Vol. 3, No. 1, (2012), 63–76.
38. Wheel, M. A., "A finite volume method for analysing the bending deformation of thick and thin plates", ***Computer Methods in Applied Mechanics and Engineering***, Vol. 147, No. 96, (1997), 199–208.
39. Amraei, A. and Fallah, N., "A development in the finite volume method for the crack growth analysis without global remeshing", ***International Journal of Engineering - Transactions A: Basics***, Vol. 29, No. 7, (2016), 890–900.
40. Sabbagh-Yazdi, S. R. and Amiri-SaadatAbadi, T., "GFV solution on UTE mesh for transient modeling of concrete aging effects on thermal plane strains during construction of gravity dam", ***Applied Mathematical Modelling***, Vol. 37, No. 1–2, (2013), 82–101.
41. Kargarnovin, M. H., Toussi, H. E., and Fariborz, S. J., "Elasto-plastic element-free Galerkin method", ***Computational Mechanics***, Vol. 33, No. 3, (2004), 206–214.
42. Passieux, J.C., Réthoré, J., Gravouil, A. and Baietto, M.C., "Local / global non-intrusive crack propagation simulation using a multigrid X-FEM solver", ***Computational Mechanics, Springer Verlag***, Vol. 52, No. 6, (2013), 1381–1393.
43. Küttler, U. and Wall, W. A., "Fixed-point fluid-structure interaction solvers with dynamic relaxation", ***Computational Mechanics***, Vol. 43, No. 1, (2008), 61–72.
44. Peng, M., Li, D., and Cheng, Y., "The complex variable element-free Galerkin (CVEFG) method for elasto-plasticity problems", ***Engineering Structures***, Vol. 33, No. 1, (2011), 127–135.
45. Ma, J., Xin, X. J., and Krishnaswami, P., "Elastoplastic meshless integral method", ***Computer Methods in Applied Mechanics and Engineering***, Vol. 197, No. 51–52, (2008), 4774–4788.

Coupling Nonlinear Element Free Galerkin and Linear Galerkin Finite Volume Solver for 2D Modeling of Local Plasticity in Structural Material

S. R. Sabbagh-Yazdi, H. Najar-Nobari

Department of Civil Engineering, KNToosi University of Technology, Tehran, Iran

P A P E R I N F O

Paper history:
Received 22 October 2019
Received in revised form 09 December 2019
Accepted 17 January 2020

Keywords:
Iterative Global/Local Method
Matrix-Free Galerkin Finite Volume Method
Non-intrusive Coupling
Nonlinear Element-Free Galerkin
Overlapping Multi-grid Patch

چکیده

این مقاله یک تکنیک عددی برای حل ترکیبی مسائلی که دامنه‌ی آنها عمدتاً الاستیک است و بخش کوچکی از دامنه‌ی آنها وارد محدوده‌ی غیرخطی شده باشد، ارائه نموده است. بر این اساس، روش گالرکین حجم محدود خطی (GFVM) با دقت و سرعت مناسب برای تحلیل الاستیک کل حوزه و روش بدون المان غیرخطی گالرکین (EFG) برای تحلیل الاستوپلاستیک به‌صورت موضعی مورد استفاده قرار گرفته است. تحلیل فوق با توجه به اختلاف بنیادین معادلات حل در هر روش، به‌صورت غیرداخل‌شونده بر اساس الگوریتم‌های چندشبکه‌ای، تفکیک دامنه و کلی–جزئی صورت گرفته است و بر اساس آن، گره‌های روش بدون المان غیرخطی (دامنه محلی) به صورت یک شبکه‌ی ریزتر در نواحی غیرخطی روی دامنه‌ی GFVM (دامنه کلی) هم‌پوشانی می‌شود. این الگوریتم بدون هیچ گونه تغییر در شبکه و یا دست‌کاری در فرمول‌بندی پایه، اقدام به تحلیل غیرخطی در بستر الاستیک خطی می‌نماید. تبادل اطلاعات بین این دو شبکه از طریق اپراتورهای خاص و با کمک تقریب حداقل مربعات متحرک (MLS) روی فصل مشترک انجام می‌گیرد. با توجه به ماهیت تکراری حل، به منظور افزایش نرخ هم‌گرایی، از شتاب دهنده‌های مختلف شبه نیوتنی (Quasi-Newtonian) و دینامیکی (Aitken's Δ^2) استفاده شده است و یک نسخه‌ی جدید از شتاب دهنده‌ی شبه نیوتنی که به جای ماتریس سختی بر اساس ماتریس رفتاری هر المان می‌باشد نیز ارائه و بررسی گردیده است. همچنین، مثال‌های عددی متعددی روی صفحات دوبعدی دارای سوراخ و یا دارای لبه‌های تیز مد نظر قرار گرفته است.

***doi**:10.5829/ije.2020.33.03c.03*